The EMBO Journal (2005) 24, 3681–3689 | © 2005 European Molecular Biology Organization | All Rights Reserved 0261-4189/05
www.embojournal.org

THE EMBO JOURNAL

Nup50/Npap60 function in nuclear protein import complex disassembly and importin recycling

Yoshiyuki Matsuura[1,2] and Murray Stewart[1,*]

[1]MRC Laboratory of Molecular Biology, Cambridge, UK and [2]Division of Biological Science, Graduate School of Science, Nagoya University, Furo-cho, Chikusa-ku, Nagoya, Japan

Nuclear import of proteins containing classical nuclear localization signals (NLS) is mediated by the importin-α:β complex that binds cargo in the cytoplasm and facilitates its passage through nuclear pores, after which nuclear RanGTP dissociates the import complex and the importins are recycled. In vertebrates, import is stimulated by nucleoporin Nup50, which has been proposed to accompany the import complex through nuclear pores. However, we show here that the Nup50 N-terminal domain actively displaces NLSs from importin-α, which would be more consistent with Nup50 functioning to coordinate import complex disassembly and importin recycling. The crystal structure of the importin-α:Nup50 complex shows that Nup50 binds at two sites on importin-α. One site overlaps the secondary NLS-binding site, whereas the second extends along the importin-α C-terminus. Mutagenesis indicates that interaction at both sites is required for Nup50 to displace NLSs. The Cse1p:Kap60p:RanGTP complex structure suggests how Nup50 is then displaced on formation of the importin-α export complex. These results provide a rationale for understanding the series of interactions that orchestrate the terminal steps of nuclear protein import.

The EMBO Journal (2005) **24,** 3681–3689. doi:10.1038/sj.emboj.7600843; Published online 13 October 2005
Subject Categories: membranes & transport; structural biology
Keywords: importin; NLS; nuclear pore; Nup50; Nup2p

Introduction

Eukaryotic cells have intricate machinery to transport macromolecules in and out of the nucleus through nuclear pore complexes (NPCs), huge supramolecular assemblies, which in vertebrates are composed of multiple copies of about 30 nucleoporins (Cronshaw *et al*, 2002) and have a mass of ~125 MDa (Fahrenkrog and Aebi, 2003). NPCs allow passive diffusion of ions and small molecules across the nuclear envelope and selectively facilitate the active transport of macromolecules when complexed with carrier proteins (importins or exportins). The majority of transport pathways are orchestrated by Ran, which exists as RanGTP in the nucleus, but RanGDP in the cytoplasm, as a consequence of the asymmetric distribution of RanGEF and RanGAP that are localized exclusively to the nucleus and cytoplasm, respectively (reviewed by Weis, 2003). Nuclear import cargoes are recognized by importins in the cytoplasm, translocated through NPCs, and released from importins by RanGTP in the nucleus. Conversely, nuclear export cargoes bind exportins only in the presence of RanGTP in the nucleus and, after passage through NPCs, the export complexes are disassembled in the cytoplasm upon RanGTP hydrolysis. Nuclear import of cargoes bearing a classical nuclear localization signal (NLS) is mediated by the importin-α:β heterodimer (Kap60p:Kap95p in yeast). Importin-α is constructed from 10 tandem Armadillo (ARM) repeats, whereas importin-β is constructed from similar HEAT repeats (Conti *et al*, 1998; Cingolani *et al*, 1999). The NLS binds to the importin-α adaptor that itself binds to importin-β via its importin-β-binding domain (IBB). Passage through NPCs is facilitated by interactions between importin-β and nucleoporins. After disassembly by nuclear RanGTP, importin-β (Kap95p in yeast) returns to the cytoplasm complexed with RanGTP, whereas the nuclear export of NLS-free importin-α (Kap60p in yeast) is mediated by the exportin CAS (Cse1p in yeast) complexed with RanGTP (reviewed by Weis, 2003).

Nuclear import complex disassembly and importin recycling involves an intricate series of steps to ensure fidelity and also to prevent futile transport cycles. Moreover, the affinities of many of these components are in the nM range, and so active displacement mechanisms are often required to facilitate their dissociation. Although structures of importin-α and -β, as well as several of their complexes, have established the mechanism of the assembly of the NLS:importin-α:β nuclear import complex (Conti *et al*, 1998; Cingolani *et al*, 1999; Kobe, 1999; Conti and Kuriyan, 2000; Fontes *et al*, 2000), its disassembly by nuclear RanGTP (Vetter *et al*, 1999; Lee *et al*, 2005) and the recycling of importin-α to the cytoplasm (Matsuura and Stewart, 2004) are less clear, especially regarding the way in which these steps are orchestrated and the roles of NPC proteins (nucleoporins). The way import or export complexes interact with NPCs and the mechanism by which this interaction contributes to translocation are poorly understood, albeit there is direct evidence for the importance of the interaction between importin-β and the FG repeats commonly found in many nucleoporins for nuclear import (Bayliss *et al*, 2000, 2002). However, interactions between import/export complexes and nucleoporins appear primarily to facilitate transport through NPCs rather than impose directionality (Weis, 2003; Zeitler and Weis, 2004). Instead, directionality is imposed by the dissociation of cargo:carrier complexes, with energy ultimately being provided by Ran-mediated GTP hydrolysis (Görlich *et al*, 2003).

In yeast, nucleoporin Nup2p appears to orchestrate the carefully choreographed series of interactions with NPC

*Corresponding author. MRC Laboratory of Molecular Biology, Hills Road, Cambridge CB2 2QH, UK. Tel.: +44 1223 402463; Fax: +44 1223 213556; E-mail: ms@mrc-lmb.cam.ac.uk

Received: 1 June 2005; accepted: 20 September 2005; published online: 13 October 2005

components involved in import complex disassembly, importin recycling and in the prevention of futile cycles resulting from components being recycled before cargo was released (Hood *et al*, 2000; Solsbacher *et al*, 2000; Gilchrist *et al*, 2002; Gilchrist and Rexach, 2003; Matsuura *et al*, 2003). Less information is available in metazoans, although vertebrate Nup50 (also called Npap60), which has some analogies to both Nup2p and RanBP3, has been proposed to act as a cofactor for importin-α:β nuclear import, as well as a component of the importin complex and thereby to stimulate importin-α:β-mediated import of classical NLSs (Lindsay *et al*, 2002). Thus, Nup50 is not simply another importin-α nuclear import cargo.

We show here that the N-terminal domain of Nup50 (residues 1–109) is able to actively displace NLSs from importin-α, indicating that Nup50 probably functions to coordinate import complex disassembly rather than chaperone the import complex through NPCs. The crystal structure of the importin-α:Nup50 complex at 2.2 Å resolution shows that Nup50 binds to two sites on importin-α: one site partially overlaps the secondary NLS-binding site located at ARM repeats 6–9 in a similar way to Nup2p (Matsuura *et al*, 2003); whereas the second Nup50-binding site overlaps with the binding site for CAS (Cse1p) and RanGTP. The structure of this complex together with that of the Cse1p:Kap60p:RanGTP complex (Matsuura and Stewart, 2004) indicates how CAS(Cse1p):RanGTP and the IBB domain cooperate to release importin-α (Kap60p) from Nup50 (Nup2p), and strongly supports Nup50 functioning primarily at the terminal stages of nuclear protein import to coordinate import complex disassembly and importin recycling.

Results

Nup50 actively displaces NLSs from importin-α

Lindsay *et al* (2002) showed that the N-terminal domain of Nup50 binds to full-length importin-α. Using a quantitative solid-phase binding assay, we found that the N-terminal domain of Nup50 (residues 1–109) binds the ARM repeat region of mouse importin-α (residues 70–529; ΔIBB importin-α) with nM affinity, whereas the affinity of NLSs to the same domain of importin-α (Figure 1A, Table I) was slightly lower

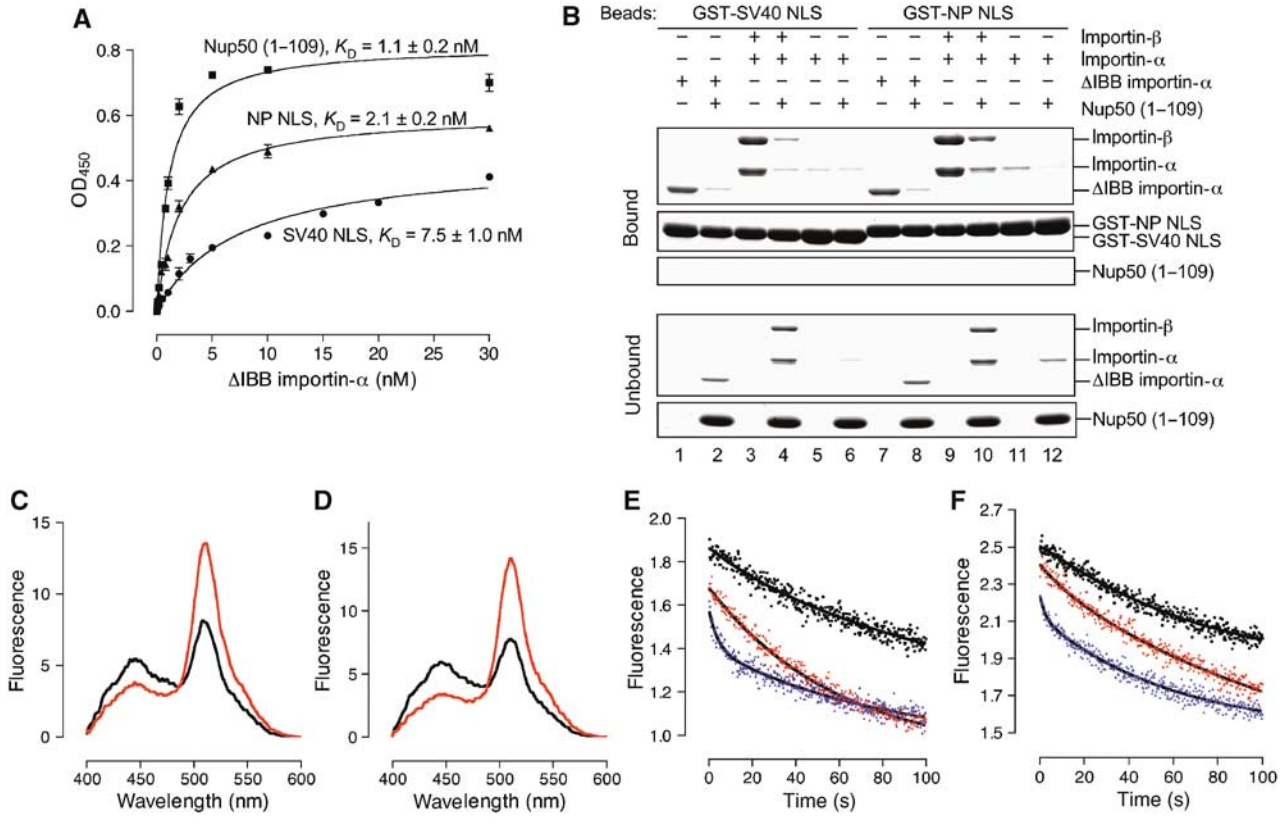

Figure 1 Nup50 displaces classical NLSs from importin-α. (**A**) Solid phase binding assay with GST-Nup50 (residues 1–109) or NLS-GFP immobilized on the microtitre plate. Each data point was performed in duplicate and error bars represent s.e.m. NP stands for nucleoplasmin. (**B**) Pulldown competition assays. Immobilized GST-SV40 NLS (lanes 1–6) or GST-NP NLS (lanes 7–12) was incubated with 6.6 μM ΔIBB importin-α (lanes 1, 2, 7, and 8), or with 8 μM importins α and β (lanes 3, 4, 9, and 10), or with 37 μM importin-α alone (lanes 5, 6, 11, and 12), unbound material washed away and then treated with buffer alone (lanes 1, 3, 5, 7, 9, and 11) or with 20 μM Nup50 (residues 1–109) (lanes 2, 4, 6, 8, 10, and 12). (**C**) Equilibrium competition between Nup50 and the monopartite SV40 NLS in solution. Emission profiles of 0.2 μM BFP-ΔIBB importin-α and 0.2 μM SV40 NLS-GFP with (black) or without (red) 1 μM Nup50 (residues 1–109). (**D**) Equilibrium competition between Nup50 and the bipartite NP NLS in solution. Emission profiles of 0.2 μM BFP-ΔIBB importin-α and 0.2 μM NP NLS-GFP with (black) or without (red) 1 μM Nup50 (residues 1–109). (**E**) Stopped-flow traces following the dissociation kinetics of SV40 NLS from importin-α, 0.2 μM BFP-ΔIBB importin-α and 0.2 μM SV40 NLS-GFP alone (black points), or with 4 μM ΔIBB importin-α (red points), or with 1 μM Nup50 (residues 109) (blue points). Fitted exponential curves are superimposed. (**F**) Stopped-flow traces following the dissociation kinetics of NP NLS from importin-α, 0.2 μM BFP-ΔIBB importin-α and 0.2 μM NP NLS-GFP alone (black points), or with 4 μM ΔIBB importin-α (red points), or with 1 μM Nup50 (residues 109) (blue points). Fitted exponential curves are superimposed.

Table I Dissociation constants determined by microtitre plate binding assay

Importin-α /Kap60p constructs	Binding partner	K_D (nM)
ΔIBB importin-α (70–529)	GST-Nup50 (1–109) wild type	1.1±0.2
ΔIBB importin-α (70–529)	GST-Nup50 (1–109) K3E/R4D	16±2
ΔIBB importin-α (70–529)	GST-Nup50 (1–109) R38A/R45D	1000±600
ΔIBB importin-α (70–529)	SV40 NLS-GFP	7.5±1.0
ΔIBB importin-α (70–529)	NP NLS-GFP	2.1±0.2
ΔIBB importin-α (70–529)	GST	Not detectable
ΔIBB importin-α (70–529)	GFP	Not detectable
ΔIBB Kap60p (88–542)	GST-Nup2p (1–51) wild type	2.0±0.2
ΔIBB Kap60p (88–542)	GST-Nup2p (1–51) K3E/R4D	16±2
ΔIBB Kap60p (88–542)	GST-Nup2p (1–51) R38A/R39A/R46A/R47A	1100±600
ΔIBB Kap60p (88–542)	GST	Not detectable

Data represent the best fit value±standard error. Each assay was performed in duplicate.

and comparable to the affinities observed by others (Fanara *et al*, 2000; Catimel *et al*, 2001; Hodel *et al*, 2001) that ranged from 9 to 17 nM. These data indicated that Nup50 binding was potentially strong enough to influence NLS binding. Indeed, a pulldown assay showed that the binding of Nup50 (residues 1–109) and the binding of NLSs to ΔIBB importin-α are mutually exclusive (Figure 1B, lanes 1, 2, 7, and 8). Likewise, Nup50 (residues 1–109) competed with NLSs for the binding to the importin-α:β complex (Figure 1B, lanes 3, 4, 9, and 10). Therefore, the ΔIBB importin-α is a good analogue of the importin-α:β complex with respect to the effect of Nup50 N-terminus on NLS binding. The binding of full-length importin-α to a monopartite NLS (SV40) was very weak, indicating that the IBB domain may be powerful enough to release monopartite cargoes (Figure 1B, lanes 5 and 6). However, the binding of full-length importin-α to a bipartite nucleoplasmin (NP) (NLS) was stronger than its binding to the SV40 NLS, and Nup50 (residues 1–109) clearly reduced the binding of full-length importin-α (Figure 1B, lanes 11 and 12). These results, together with the nucleoplasmically oriented localization of Nup50 (Guan *et al*, 2000), raised a possibility that Nup50 promotes the disassembly of nuclear protein import complex at the nucleoplasmic side of the nuclear pore.

We used a FRET assay (Matsuura *et al*, 2003) that specifically detects the binding of NLS to importin-α (Kap60p) to evaluate the ability of Nup50 to actively displace NLSs. To do this, we used ΔIBB importin-α construct because it behaved in essentially the same way as the importin-α:β complex in the equilibrium competition assay (Figure 1B), and also because this system has been shown previously (Matsuura *et al*, 2003) to measure the kinetics of NLS dissociation reliably. A BFP-GFP FRET signal was observed when NLS-GFP was added to BFP-ΔIBB importin-α (Figure 1C and D). The FRET signal decreased to the background in the presence of Nup50 (residues 1–109), demonstrating that Nup50 can compete with both the monopartite SV40 NLS (Figure 1C) and the bipartite NP NLS (Figure 1D). Stopped-flow experiments showed that the rate of NLS dissociation in the presence of Nup50 was an order of magnitude higher than the rate of spontaneous dissociation of NLSs (Figure 1E and F; Table II). Although this was not as large as the increase in rate observed with Nup2p under analogous conditions (Matsuura *et al*, 2003), it still indicated that Nup50 was functioning in a similar manner and produced a substantial increase in the rate of the release of NLSs by an active displacement mechanism, suggesting that the function of Nup50/Nup2p in accelerating NLS release in the terminal stages of nuclear import (Gilchrist *et al*, 2002; Matsuura *et al*, 2003) is conserved from yeast to vertebrates.

Table II Nup50 accelerates the off-rate of NLSs from importin-α

NLS	Spontaneous dissociation (s^{-1})	Nup50-accelerated release (s^{-1})
SV40	0.027±0.001	0.40±0.06
Nucleoplasmin	0.0122±0.0003	0.45±0.02

Data represent mean±standard error based on four measurements.

Nup50 binds to two sites on importin-α

To understand how Nup50 works, we obtained crystals of a complex between mouse importin-α (residues 70–529) and mouse Nup50 (residues 1–109) that diffracted to 2.2 Å resolution using synchrotron radiation. Molecular replacement using the ARM repeats of importin-α (Kobe, 1999) showed a clear tube of difference density. The side chains and main chain carbonyls were well defined and residues 1–46 of Nup50 were traced unambiguously (Figure 2A). Refinement yielded a final model of the complex with R_{free} 25.4% (R_{cryst} 22.1%) and good stereochemistry (Table III).

Nup50 residues 1–46 bind intimately along the surface of importin-α and bury 4377 $Å^2$ of interfacial surface area, consistent with their nM affinity. The N-terminus of Nup50 (residues 1–15; binding segment 1) extends along the gently twisting NLS-binding groove on the inner surface of the importin-α ARM repeats in a direction antiparallel to that of importin-α in the ARM domain. The N-terminal cluster of basic residues (Lys3 and Arg4) of Nup50 bind to the minor NLS binding site in the same way as NLS-containing cargoes (Conti and Kuriyan, 2000; Fontes *et al*, 2000). Nup50 residues 11–15 (^{11}TDRNW^{15}) form a β-turn that packs against the central part of the inner surface of importin-α, which partially overlaps with the major NLS-binding site. After this β-turn, the path of Nup50 extends towards the importin-α C-terminus, and Nup50 residues 24–46 (binding segment 2) wrap around the outer surface of ARM9–10. Nup50 Met24 and Phe27 insert into hydrophobic pockets on the outer surface of ARM9 (see the electrostatically neutral surface on importin-α in Figure 2B). Nup50 residues 31–36 (^{31}SEEVMK^{36}) form two turns of α-helix that direct Nup50 residues 37–46, rich in basic residues, towards the highly acidic surface on ARM10 (Figure 2B). Thus, the interaction between Nup50 and the C-terminus of importin-α seems to be mainly electrostatic. The

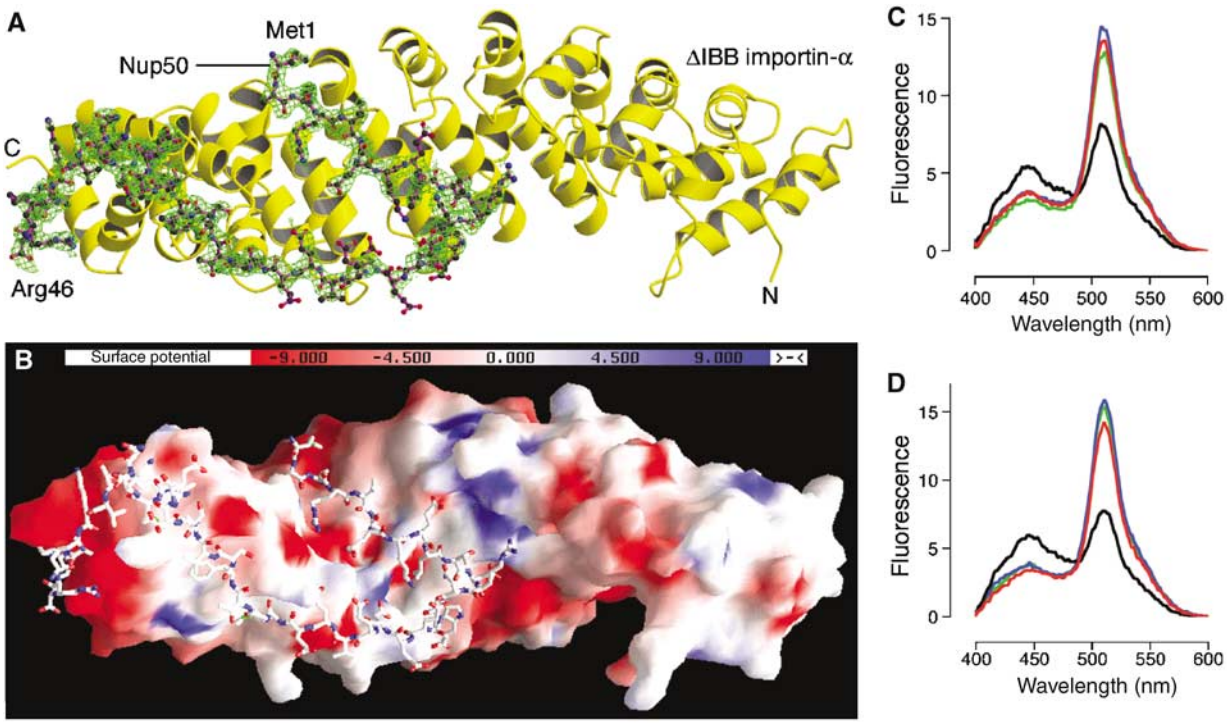

Figure 2 Crystal structure of the Nup50:importin-α complex and competition assays using structure-based mutants showed that Nup50 binds at two sites on importin-α, and the NLS displacement by Nup50 requires interaction with both sites on importin-α. (**A**) Overview of the Nup50:importin-α complex with the $2F_o-F_c$ map around Nup50 contoured at 1σ superimposed. Nup50 residues are shown in ball-and-stick format. (**B**) Electrostatic potential on importin-α, with Nup50 removed, shaded from −9 kT/e (red) to +9 kT/e (blue) calculated using GRASP (Nicholls *et al*, 1991). (**C**) FRET-based competition assay. Emission profiles of 0.2 μM BFP-ΔIBB importin-α and 0.2 μM SV40 NLS-GFP without (red) 1 μM Nup50 (residues 1–109) or with (black) 1 μM Nup50 (residues 1–109, wild type) or with (blue) 1 μM Nup50 (residues 1–109, K3E/R4D), or with (green) 1 μM Nup50 (residues 1–109, R38A/R45D). (**D**) FRET-based competition assay. Emission profiles of 0.2 μM BFP-ΔIBB importin-α and 0.2 μM NP NLS-GFP without (red) 1 μM Nup50 (residues 1–109) or with (black) 1 μM Nup50 (residues 1–109, wild type) or with (blue) 1 μM Nup50 (residues 1–109, K3E/R4D) or with (green) 1 μM Nup50 (residues 1–109, R38A/R45D).

Table III Crystallographic statistics

Data collection statistics	
Space group	$P4_12_12$
Unit cell dimensions (Å)	$a=b=74.47$, $c=188.02$
Resolution range (Å)[a]	100–2.2 (2.32–2.20)
Wilson *B*-factor	43.7
Total observations[a]	207 778 (16 676)
Unique reflections[a]	27 445 (3727)
Completeness (%)[a]	98.9 (94.9)
R_{merge} (%)[a]	10.0 (43.8)
I/σ[a]	5.5 (1.9)
Refinement statistics	
Number of reflections (working, test)	26 000/1377
R_{cryst}/R_{free} (%)	22.1/25.4
Total number of non-H atoms	3728
Number of water molecules	116
R.m.s. deviation from ideal bond length (Å)	0.006
R.m.s. deviation from ideal bond angles (deg)	1.150
Ramachandran plot (%)	
Core region	93.8
Allowed region	5.7
Generously allowed region	0.2
Disallowed region	0.2

[a]Parentheses refer to final resolution shell.

binding of Nup50 segment 2 to ARM9–10 is consistent with a fragment of importin-α that contained residues 396–521 still binding Nup50 (Lindsay *et al*, 2002). Moreover, ionic interactions involving the basic residues in segment 2 (^{41}KKAKRR^{46}) with acidic residues in importin-α are clearly crucial to this interaction, consistent with the observation that, when these basic residues were mutated to Ala, binding to Nup50 was undetectable (Lindsay *et al*, 2002). Nup50 residues 16–23 that connect the two binding segments are rich in acidic residues and, although the connectivity of the main chain was clear, the side chain density was not well defined (Figure 2A), and so these residues probably function as a flexible linker connecting the two binding segments. Residues 47–109 of Nup50 were not visible and were probably disordered in the crystal, possibly because this region of Nup50 is rich in glycine.

NLS displacement by Nup50 requires interaction with both sites on importin-α

Mutagenesis indicated that it is functionally important that Nup50 interacts with both sites on importin-α. As shown in Figure 1C and D, the FRET signal that results when GFP fusions to monopartite or bipartite NLSs bind to BFP-importin-α is dramatically reduced when the GFP-NLS is displaced by Nup50. However, as shown in Figure 2C and D, Nup50 constructs in which the key basic residues in either the first (K3E/R4D) or the second (R38A/R45D) importin-α-binding site were mutated were unable to displace either type of NLS, and the FRET signal remained unaltered. Mutations at the first site (K3E/R4D) reduced, but did not eliminate, the affinity of Nup50(1–109) for importin-α, whereas mutations

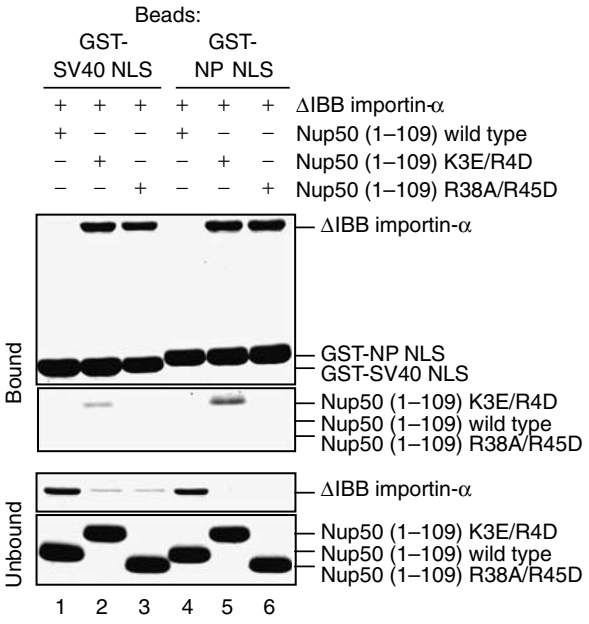

Figure 3 Pulldown competition assay. Immobilized GST-SV40 NLS (lanes 1–3) or GST-NP NLS (lanes 4–6) was incubated with 6.6 μM ΔIBB importin-α, unbound protein washed away and then treated with 20 μM Nup50 (residues 1–109, wild type) (lanes 1 and 4) or with 20 μM Nup50 (residues 1–109, K3E/R4D) (lanes 2 and 5), or with 20 μM Nup50 (residues 1–109, R38A/R45D) (lanes 3 and 6).

at the second site (R38A/R45D) dramatically reduced the affinity by three orders of magnitude (Table I). Therefore, the second binding site has higher affinity and is crucial for the binding. Consistent with this, a pulldown competition assay showed that the K3E/R4D mutant of Nup50 bound to ΔIBB importin-α:NLS complexes, but was unable to displace NLSs, whereas the R38A/R45D mutant of Nup50 did not form a trimeric complex with ΔIBB importin-α and NLSs, and did not displace NLSs (Figure 3). Taken together, these results suggest a two-step mechanism of NLS displacement, whereby the second binding site of Nup50 binds to the importin-α C-terminus first, and then the first binding site of Nup50 pushes out NLSs from the central groove of importin-α.

Yeast Kap60p:Nup2p complex

The electron density observed in the mouse importin-α:Nup50 complex along the NLS-binding groove was remarkably similar to the difference density observed in the yeast Kap60p:Nup2p (residues 1–51) complex (Matsuura *et al*, 2003). The Nup2p complex crystals also showed positive density on the surface of ARM9–10, which was similar to the Nup50 density on the C-terminus of importin-α. This density was originally interpreted as the Kap60p C-terminus, but the poor quality in this region of the 2.6 Å resolution density map in the Nup2p complex crystals frustrated attempts to unambiguously assign amino-acid residues, and even the direction of main chain in this region was not clear. The higher quality of the 2.2 Å resolution structure of the importin-α:Nup50 complex, the similarity in the appearance of the density map in both crystals, and the high level of sequence conservation between yeast Nup2p and mouse Nup50 at their N-termini (Figure 4C) prompted us to revisit the Nup2p structure. We found that it was indeed possible to trace the Nup2p chain along the surface of Kap60p, following essentially the same path as Nup50 binds along importin-α. Placing the conserved residues at equivalent positions (Figure 4A) resulted in a modest decrease in R_{free} from 25.7 to 25.1%. From the crystallographic data alone, it was not possible to distinguish unequivocally between the previous model (Matsuura *et al*, 2003) and this revised model, because side chain density was only unambiguous for the basic residues at the beginning and end of the region that bind along the inner groove of importin-α, and were common to both sequences (see Supplementary Figure 1). Unfortunately, the side chain density for the residues in the middle of this region in which the sequences differed were poorly resolved in the Nup2p:Kap60p structure, although the sequence conservation and the high quality of Nup50 structure suggest that the revised model for Nup2p binding to Kap60p is more plausible. We therefore used Nup2p mutants to distinguish between the two models. As shown in Figure 4D and E, Nup2p mutants (K3E/R4D and R38A/R39A/R46A/R47A) analogous to those in the two binding domains of Nup50 (see Figure 2) also failed to displace monopartite or bipartite NLSs from Kap60p, making it very likely that both proteins are functioning by similar two-site mechanisms and that the regions originally identified as Nup2p residues 36–51 and Kap60p residues 510–526 are indeed Nup2p residues 2–18 and 28–46, respectively. Binding studies (Table I) indicated that, similar to Nup50, the second binding site of Nup2p had higher affinity for Kap60p.

Structural basis for the CAS(Cse1p):RanGTP-mediated release of importin-α from Nup50 (Nup2p)

The structure of the Cse1p:Kap60p:RanGTP complex (Matsuura and Stewart, 2004) showed that Cse1p:RanGTP binds to both the IBB domain and the C-terminus of Kap60p, and that the assembly of this ternary complex requires that the IBB domain is bound along the NLS-binding sites on Kap60p. Superimposing the importin-α:Nup50 and Kap60p:Nup2p structures on the Cse1p:Kap60p:RanGTP complex indicated that the N-terminal binding segment 1 of Nup50 and Nup2p would clash with the IBB domain, and binding segment 2 of Nup50 and Nup2p would clash with Cse1p on ARM repeat 9 of importin-α/Kap60p and RanGTP on ARM10 (Figure 5). Thus, Nup50 and Nup2p bind to importin-α/Kap60p at sites critical for the assembly of the ternary export complex, and this explains why Nup50 competes with CAS:RanGTP for binding to importin-α (Lindsay *et al*, 2002) and also why Cse1p:RanGTP and the IBB domain cooperate to release Kap60p from Nup2p (Matsuura *et al*, 2003).

Discussion

We have determined the crystal structure of the mouse importin-α:Nup50 complex and showed that the binding site for residues 1–15 (binding segment 1) of Nup50 overlaps with the importin-α NLS-binding sites in a manner analogous to that observed for yeast Nup2p binding to Kap60p. A FRET-based stopped-flow assay confirmed that Nup50 actively displaces NLSs from importin-α. Moreover, in addition to interacting along the NLS-binding groove of importin-α, the Nup50-binding site also extends along the outer surface of the C-terminal part of importin-α, interacting with ARM repeats 9

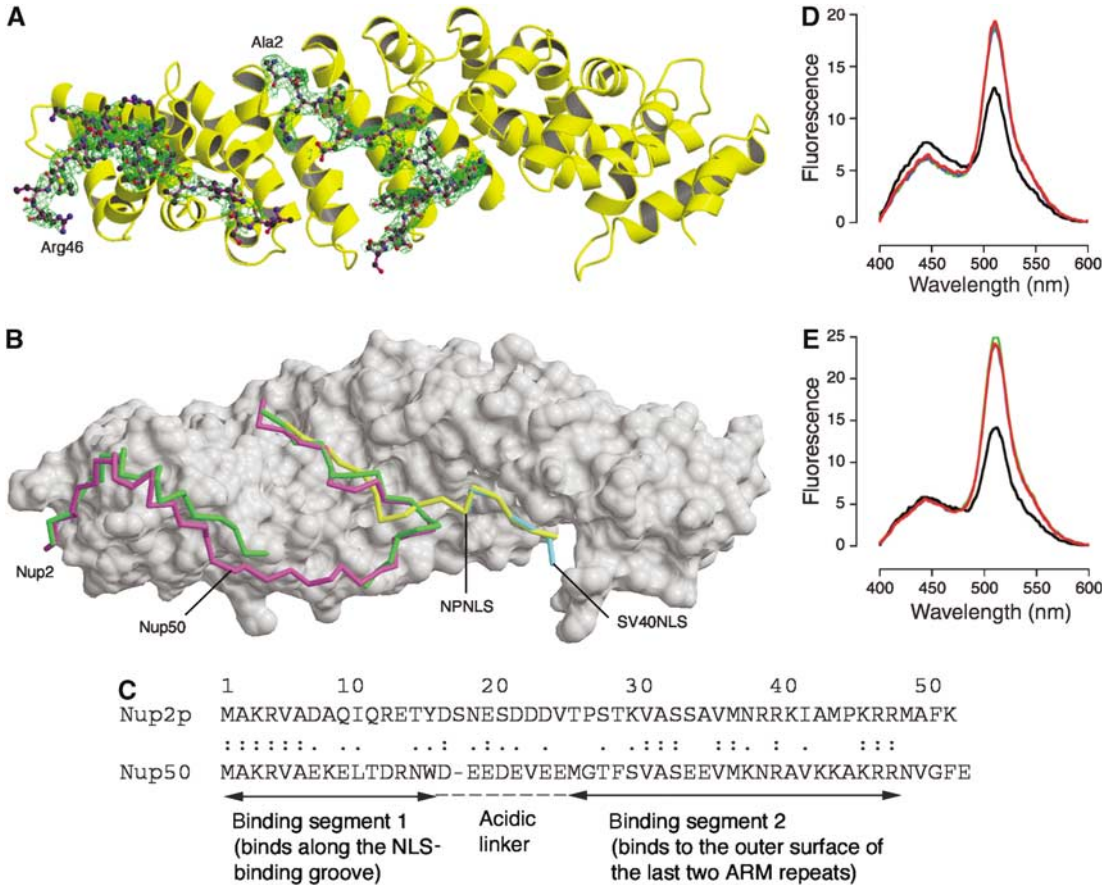

Figure 4 Conserved interactions between Nup50 (Nup2p) and importin-α (Kap60p). (**A**) Revised model of the ΔIBB-Kap60p:Nup2p (residues 1–51) complex with the $2F_o-F_c$ map around Nup2p contoured at 1σ superimposed. Nup2p residues are shown in ball-and-stick format. (**B**) Superimposition of the main chains of Nup50 (magenta), Nup2p (green), SV40 NLS (cyan), and NP NLS (yellow) on the surface of ΔIBB importin-α. (**C**) Sequence alignment of yeast Nup2p and mouse Nup50 at the N-terminal importin-α-binding domain. (**D**) Mutants in the Nup2p residues analogous to those identified in the two importin-α-binding regions of Nup50 do not displace the monopartite or bipartite NLSs from yeast importin-α (Kap60p). Emission profiles of 0.2 μM BFP-ΔIBB-Kap60p and 0.2 μM SV40 NLS-GFP without (red) 2 μM Nup2p (residues 1–51) or with (black) 2 μM Nup2p (residues 1–51, wild type) or with (blue) 2 μM Nup2p (residues 1–51, K3E/R4D), or with (green) 2 μM Nup2p (residues 1–51, R38A/R39A/R46A/R47A). (**E**) Emission profiles of 0.2 μM BFP-ΔIBB-Kap60p and 0.2 μM NP NLS-GFP without (red) 2 μM Nup2p (residues 1–51) or with (black) 2 μM Nup2p (residues 1–51, wild type) or with (blue) 2 μM Nup2p (residues 1–51, K3E/R4D), or with (green) 2 μM Nup2p (residues 1–51, R38A/R39A/R46A/R47A).

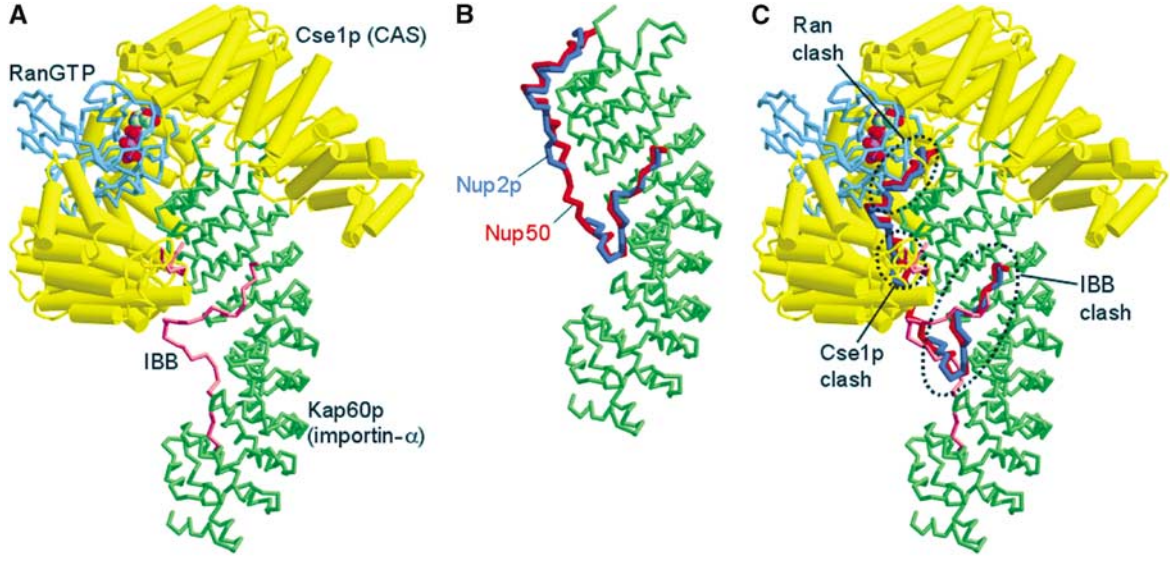

Figure 5 Nup50 (Nup2p) binds to sites crucial for the formation of nuclear export complex of importin-α (Kap60p) with CAS (Cse1p) and RanGTP. (**A**) The Cse1p:Kap60p:RanGTP complex (Matsuura and Stewart, 2004). (**B**) Nup50 (red) and Nup2p (blue) are superimposed on the Kap60p ARM repeats in the Cse1p:Kap60p:RanGTP complex. (**C**) (A) and (B) superimposed. Cse1p, yellow; Ran, light blue; Kap60p IBB, pink; Kap60p ARM repeats, green. GTP is shown as space-filling model.

and 10. Comparison with the Cse1p:Kap60p:RanGTP complex showed that Nup50 and Nup2p bind at a site that is crucial for assembly of the importin-α export complex. Therefore, our results provide a structural rationale for understanding the competition between Nup50 (Nup2p) and classical NLSs or between these nucleoporins and CAS(Cse1p):RanGTP for binding to importin-α(Kap60p), and strongly suggest that these functions are conserved from yeast to vertebrates.

It is likely that Nup50 and Nup2p promote nuclear protein import through related mechanisms. As discussed previously for Nup2p (Hood *et al*, 2000; Solsbacher *et al*, 2000; Gilchrist *et al*, 2002; Gilchrist and Rexach, 2003; Matsuura *et al*, 2003), these nucleoporins probably function as scaffolding proteins to facilitate nuclear import complex disassembly, cargo release and importin recycling by bringing the different components and RanGTP into close proximity at the nuclear basket at the NPCs' nuclear face. Figure 6 illustrates how the Nup50 (Nup2p) could accelerate nuclear import complex disassembly and importin-α recycling. In the absence of Nup50 (Nup2p), RanGTP binding to importin-β (Kap95p) generates a conformational change that releases the IBB domain (Lee *et al*, 2005), which then displaces NLS cargo from importin-α (Kap60p) (Kobe, 1999). Importin-α (Kap60p) then forms a complex with RanGTP and CAS (Cse1p) that is exported to the cytoplasm (reviewed by Weis, 2003). Nup50 (Nup2p) could accelerate this process both by increasing the local concentration of the components and also by actively displacing NLS cargo from importin-α (Kap60p). The active displacement of the NLS could occur either before or after the RanGTP-induced dissociation of the IBB domain from importin-β (Kap95p). As Nup50 (Nup2p) is able to actively displace an NLS from the ΔIBB constructs, it does not appear that the IBB domain is required for this function and so its prior dissociation from importin-β (Kap95p) is probably not necessary. Of course, both mechanisms could operate in parallel or simultaneously so that import complex disassembly occurred in concert with NLS release.

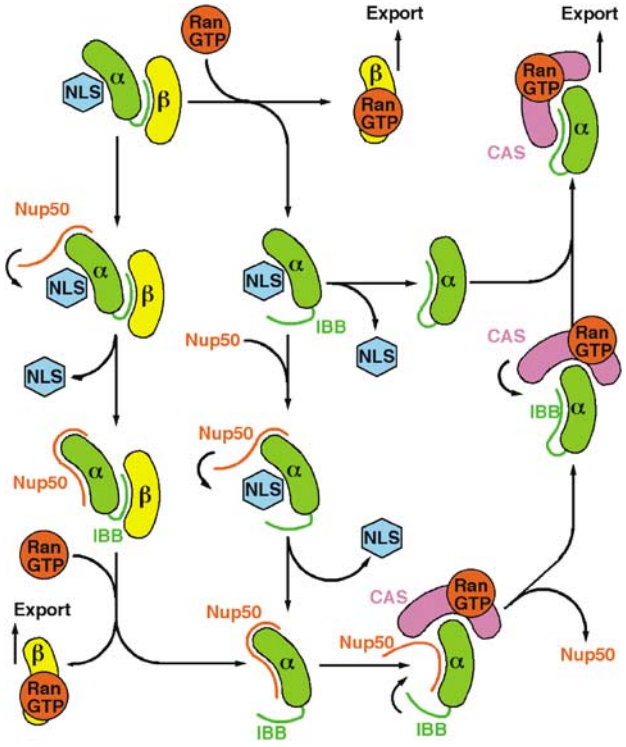

Figure 6 Schematic illustration of the possible ways in which NLS displacement and importin-α recycling could be mediated by Nup50, CAS and RanGTP. The disassembly of nuclear import complex and the assembly of nuclear export complexes could happen with or without Nup50. In the absence of Nup50, RanGTP would dissociate the IBB domain from importin-β, the NLS is released from importin-α by the IBB domain, and the cargo-free importins α and β are exported to cytoplasm separately. In the presence of Nup50, Nup50 could accelerate the NLS release and also act as a platform on which importin-α export complex is assembled. The active displacement of NLS by Nup50 probably occurs in two steps. First, Nup50 would make a transient complex with incoming importin-α–β:NLS complex by binding to the C-terminus of importin-α. The N-terminus of Nup50 would then displace NLS, and after importin-β is dissociated by RanGTP, the IBB domain, CAS and RanGTP cooperate to release importin-α from Nup50. Nup50 could also displace NLS from importin-α after the IBB domain is released from importin-β by RanGTP, and this may be important for dissociation of strongly bound bipartite cargoes for which the IBB domain alone may not be enough to achieve quick release. Thus, several parallel pathways are conceivable. These are not mutually exclusive and the presence of Nup50 at the nuclear face of the NPCs would increase the overall rate of nuclear trafficking, even though Nup50 may not be absolutely required for trafficking because of functional redundancy.

The identification of the two Nup50-binding sites suggests that the Nup50 interaction may function through a mechanism analogous to the autoinhibitory mechanism proposed for the displacement of NLSs by the importin-α IBB domain (Kobe, 1999). Thus, binding of the second segment (residues 24–46) of Nup50 to ARM repeats 9 and 10 of importin-α could anchor Nup50 and so greatly increase the local concentration of segment 1 (residues 1–15). After the NLS has been displaced by Nup50 (Nup2p), these nucleoporins are then themselves displaced from the importin-α C-terminus by CAS (Cse1p) and RanGTP binding to form the export complex. The displacement of Nup50 and Nup2p by CAS(Cse1):RanGTP could be achieved in two steps, whereby CAS(Cse1p):RanGTP would first displace binding segment 2 (Nup50 residues 24–46) from the C-terminus of importin-α. This would substantially weaken the affinity of Nup50 for importin-α and so facilitate the incorporation of the IBB domain to form a stable export complex, committing the cargo-free importin-α for nuclear export. Conformational changes in the exportin CAS (Cse1p) may also play an important role in the assembly process of the nuclear export complex (Matsuura and Stewart, 2004; Cook *et al*, 2005).

Although it seems paradoxical to displace the NLS with a protein that binds more strongly that then has itself to be released, it is likely that such a mechanism enables Nup50 (Nup2p) to act as a molecular ratchet preventing reassembly of the import complex and so preventing futile transport cycles. Moreover, although the affinity of Nup50 (Nup2p) for importin-α (Kap60p) is greater than that of NLSs or the IBB domain, this is only the case when it is bound to both sites. Once displaced from the high-affinity site at the importin-α (Kap60p) C-terminus, Nup50 (Nup2p) has greatly reduced affinity and so would be easily displaced by the IBB domain.

Our results indicate that, contrary to previous proposals (Lindsay *et al*, 2002), Nup50 displaces NLSs in a manner similar to that seen with Nup2p (Gilchrist *et al*, 2002; Matsuura *et al*, 2003). The binding of Nup50 (Nup2p) segment 2 to the importin-α (Kap60p) C-terminus would enable the formation of a transient Nup50:NLS:importin-α:β

(Nup2p:NLS:Kap60p:Kap95p) complex, followed by displacement of the NLSs, which would be consistent with the increase in NLS off-rate observed in the presence of Nup2p (Gilchrist *et al*, 2002; Matsuura *et al*, 2003). Lindsay *et al* (2002) showed that importin-α could bind an NLS and GST–GFP–Nup50 (residues 1–109) simultaneously, and this could be explained if the linker between the GFP and Nup50 was too short and the GST and GFP fused to Nup50 N-terminus weakened the binding of the first binding site of Nup50 (residues 1–15) to the NLS-binding site (note that the N- and C-termini of GFP are close to each other (Yang *et al*, 1996)). The Nup50 construct we used for the competition assays had nothing fused to its N-terminus, and instead had His-tag at the C-terminus. As it could cause premature dissociation of the importin-α–β:cargo complex, the propensity of Nup50 to displace NLSs from importin-α would seemingly imply that Nup50 should inhibit nuclear protein import if it were in contact with the import cargo:carrier complex throughout its passage through NPCs, as proposed by Lindsay *et al* (2002). However, Nup50 instead stimulates the importin-α:β-mediated import of classical NLSs (Lindsay *et al*, 2002), suggesting that the structural and biochemical properties of Nup50 are optimized to promote, rather than inhibit, nuclear trafficking. It may be possible to reconcile these seemingly contradictory observations using the kinetics of the series of interactions that occur during nuclear trafficking. The average residence time of the SV40 NLS at NPCs is about 10 ms (Yang *et al*, 2004), whereas the residence time of Nup50 at the NPCs is 20 s or longer (Rabut *et al*, 2004). Thus, the residence time of Nup50 at the NPCs is probably of the order of 2000-fold longer than that of the import cargo:carrier complex. Therefore, on the time scale of nuclear transport, Nup50 appears to leave NPCs only very occasionally and the very slow shuttling of Nup50 detected by a heterokaryon assay (Lindsay *et al*, 2002) probably reflects rapid re-import of Nup50 after occasional mislocalization to the cytoplasm. In the context of nuclear protein import, Nup50 probably functions without actually leaving NPCs, and so it is probably unlikely that Nup50 accompanies importin-α:β-cargo complex all the way from the bulk cytoplasm to the nucleus. Instead, Nup50 probably acts primarily after the importin-α:β-cargo complex docks onto the NPCs. The nucleoplasmically biased localization of Nup50 within NPCs (Guan *et al*, 2000) suggests that it functions primarily within the nucleoplasmic half of NPCs and probably mainly at the nuclear basket. In this context, it is reasonable to propose that Nup50 promotes nuclear import primarily by facilitating disassembly of the importin-α:β-cargo complex. Subsequent release of importin-α from Nup50 by CAS and RanGTP would enable Nup50 to function as a catalyst of overall transport cycle, as has been suggested for Nup2p for nuclear protein import in yeast (Hood *et al*, 2000; Solsbacher *et al*, 2000; Gilchrist *et al*, 2002; Gilchrist and Rexach, 2003; Matsuura *et al*, 2003).

In summary, we have established the structure of the Nup50:importin-α complex and shown that Nup50 actively displaces and accelerates the release of NLS-containing cargoes from importin-α. Moreover, this structure, combined with the structure of the Cse1p:Kap60p:RanGTP export complex, provides a structural rationale for the series of coordinated interactions at the nuclear basket that both disassemble the importin–cargo import complex and then recycle the importins to the cytoplasm for a further transport cycle.

Materials and methods

Preparation of importin-α:Nup50 complex for crystallization

GST-mouse Nup50 (residues 1–109) and untagged mouse importin-α (residues 70–529) were expressed in *Escherichia coli* strain BL21-Gold(DE3) (Stratagene) at 20°C overnight from pGEX-TEV (Matsuura and Stewart, 2004) and pET30a (Novagen), respectively. After harvesting, the two sets of cells were mixed, suspended in PBS, 1 mM EDTA, 2 mM DTT, 1 mM Pefabloc, and lysed by sonication on ice. All subsequent steps were performed at 4°C. Tween20 was added to 0.1%, and the clarified lysates were incubated with glutathione-Sepharose (Amersham) overnight. After washing the beads extensively with PBS, 0.1% Tween20, 2 mM β-mercaptomethanol, and 0.1 mM Pefabloc, the GST tag was removed with His-TEV protease (30 μg/ml) overnight. The importin-α (70–529):Nup50 (1–109) complex released from the resin was passed through Ni-NTA (Novagen) and finally purified over Superdex200 (Amersham) in 2 mM HEPES (pH 7.0), 150 mM NaCl, and 2 mM DTT. The complex was concentrated to 12 mg/ml using a VIVASPIN (Vivascience) concentrator (Mr 5000).

Crystallization, data collection, and structure determination

Crystals of the importin-α (70–529):Nup50 (1–109) complex were grown at 18°C from 10 mg/ml protein by hanging drop vapour diffusion against 50 mM MES (pH 6.0), 150 mM NaCl, 20.5% PEG3350, and 10 mM DTT. A $100 \times 100 \times 200\,\mu m^3$ crystal grew in 1 week. The crystal was briefly dipped in 50 mM MES (pH 6.0), 150 mM NaCl, 25% PEG3350, 12% PEG400, and 10 mM DTT, and flash-frozen by plunging into liquid N_2. The crystal had $P4_12_12$ ($a = b = 74.5$ Å, $c = 188.0$ Å) symmetry with one complex in the asymmetric unit. A 2.2-Å data set was collected at 100 K at ESRF beamline ID29 (Grenoble, France) and processed using MOSFLM and CCP4 programs (CCP4, 1994). The structure was solved by molecular replacement using CNS (Brünger *et al*, 1998) using the mouse importin-α ARM repeats (residues 70–496) (Kobe, 1999) as a model. Iterative cycles of model building (aided by ARP/wARP (Perrakis *et al*, 1999)) using O (Jones *et al*, 1991) and refinement using CNS yielded a final model with R_{free} 25.4% (R_{cryst} 22.1%) that contained importin-α residues 75–498, Nup50 residues 1–46, and 116 water molecules. Asn239 of importin-α is a Ramachandran outlier as in other mouse importin-α structures (Kobe, 1999; Fontes *et al*, 2000). Molecular graphics used Molscript (Kraulis, 1991), Raster3D (Merritt and Bacon, 1997), and MSMS.

Binding assays

His/S-mouse importin-α (residues 70–529) was expressed as described (Fontes *et al*, 2000). His/S-Nup2p (residues 1–51), His/S-Kap60p (residues 88–542), His/S-BFP-Kap60p (residues 81–542), SV40 NLS-GFP, NP NLS-GFP, GST-SV40 NLS, and GST-NP NLS were expressed as described (Matsuura *et al*, 2003). His/S-BFP-mouse importin-α (residues 70–529), importin-β and mouse Nup50 (residues 1–109)-His were expressed from pET30a. GST-Nup50 (residues 1–109) and GST-Nup2p (residues 1–51) were expressed from pGEX-TEV (Matsuura and Stewart, 2004), which has a long linker (corresponding to 20 amino acids) between the C-terminus of GST and the multi-cloning site to alleviate the steric hindrance problem caused by the GST moiety. Mutants of His/S-Nup2p (residues 1–51), Nup50 (residues 1–109)-His, GST-Nup2p (residues 1–51), and GST-Nup50 (residues 1–109) were prepared using the Quickchange system (Stratagene) and all constructs were verified by sequencing. GST-tagged proteins were purified over glutathione-Sepharose (Amersham). His-tagged proteins were purified over Ni-NTA (Novagen). Microtitre plate-binding assays and FRET-based competition assays were performed as described (Matsuura *et al*, 2003). Pulldown assays were performed in binding buffer (PBS, 0.1% Tween20, 2 mM DTT, and 0.2 mM PMSF) as described (Matsuura *et al*, 2003).

NLS dissociation kinetics

NLS dissociation kinetics were measured at 25°C in PBS with an Applied Photophysics SX18 stopped-flow spectrophotometer. BFP was excited at 360 nm, with GFP emission monitored using a 475 nm filter. Protein concentrations are those after the mixing in the stopped-flow cell. Data were fitted to double exponentials by nonlinear regression using GraphPad Prism, with one of the exponentials being a slow photobleaching term and the other representing NLS dissociation. Photobleaching was determined by fitting single exponential to the decay curve after mixing fluor-

ophores with PBS alone, and these parameters were constrained during double-exponential fitting to NLS dissociation time course. Steady-state fluorescence spectra were recorded using Perkin-Elmer LS50B spectrofluorometer at 25°C in PBS. Excitation was at 360 nm, and slit widths were 6 nm for excitation and 10 nm for emission. Samples were incubated for 1 h before measurement. GFP and BFP alone both fluoresce at 510 nm when excited at 360 nm, but in the ΔIBB importin-α:NLS complex this fluorescence is enhanced by FRET by about a factor of two. Therefore, as discussed previously (Matsuura *et al*, 2003) there is only a halving in fluorescence in the presence of a five-fold excess of Nup50 (consistent with virtually complete dissociation of the complex).

Supplementary data

Supplementary data are available at *The EMBO Journal* Online.

Acknowledgements

We thank Andrew McCarthy at ESRF for help during data collection and Bostjan Kobe (University of Queensland) and Ian Macara (University of Virginia) for the generous gifts of mouse importin-α2 cDNA and mouse Nup50 cDNA, respectively. We are grateful to our colleagues, especially Phil Evans, Andrew Leslie, Neil Marshall, and Hidemi Hirano, for their many comments, criticisms, and assistance.

Accession numbers

The coordinates of importin-α:Nup50 (1–109) complex and the revised Kap60p:Nup2p complex have been deposited in the Protein Data Bank with the accession codes 2c1m and 2c1t, respectively.

References

Bayliss R, Littlewood T, Stewart M (2000) Structural basis for the interaction between FxFG nucleoporin repeats and importin-β in nuclear trafficking. *Cell* **102:** 99–108

Bayliss R, Littlewood T, Strawn LA, Wente SR, Stewart M (2002) GLFG and FxFG nucleoporins bind to overlapping sites on importin-β. *J Biol Chem* **277:** 50597–50606

Brünger AT, Adams PD, Clore GM, DeLano WL, Gros P, Grosse-Kunstleve RW, Jiang JS, Kuszewski J, Nilges M, Pannu NS, Read RJ, Rice LM, Simonson T, Warren GL (1998) Crystallography & NMR system: a new software suite for macromolecular structure determination. *Acta Crystallogr D* **54:** 905–921

Catimel B, Teh T, Fontes MR, Jennings IG, Jans DA, Howlett GJ, Nice EC, Kobe B (2001) Biophysical characterization of interactions involving importin-α during nuclear import. *J Biol Chem* **276:** 34189–34198

Cingolani G, Petosa C, Weis K, Muller CW (1999) Structure of importin-β bound to the IBB domain of importin-α. *Nature* **399:** 221–229

Collaborative Computational Project No. 4 (1994) The CCP4 suite: programs for protein crystallography. *Acta Crystallogr D* **50:** 760–763

Conti E, Kuriyan J (2000) Crystallographic analysis of the specific yet versatile recognition of distinct nuclear localization signals by karyopherin-α. *Struct Fold Des* **8:** 329–338

Conti E, Uy M, Leighton L, Blobel G, Kuriyan J (1998) Crystallographic analysis of the recognition of a nuclear localization signal by the nuclear import factor karyopherin-α. *Cell* **94:** 193–204

Cook A, Fernandez E, Lindner D, Ebert J, Schlenstedt G, Conti E (2005) The structure of the nuclear export receptor Cse1 in its cytosolic state reveals a closed conformation incompatible with cargo binding. *Mol Cell* **18:** 355–367

Cronshaw JM, Krutchinsky AN, Zhang W, Chait BT, Matunis MJ (2002) Proteomic analysis of the mammalian nuclear pore complex. *J Cell Biol* **158:** 915–927

Fahrenkrog B, Aebi U (2003) The nuclear pore complex: nucleocytoplasmic transport and beyond. *Nat Rev Mol Cell Biol* **4:** 757–766

Fanara P, Hodel MR, Corbett AH, Hodel AE (2000) Quantitative analysis of nuclear localization signal (NLS)-importin-α interaction through fluorescence depolarization. Evidence for auto-inhibitory regulation of NLS binding. *J Biol Chem* **275:** 21218–21223

Fontes MR, Teh T, Kobe B (2000) Structural basis of recognition of monopartite and bipartite nuclear localization sequences by mammalian importin-α. *J Mol Biol* **297:** 1183–1194

Gilchrist D, Mykytka B, Rexach M (2002) Accelerating the rate of disassembly of karyopherin:cargo complexes. *J Biol Chem* **277:** 18161–18172

Gilchrist D, Rexach M (2003) Molecular basis for the rapid dissociation of nuclear localization signals from karyopherin α in the nucleoplasm. *J Biol Chem* **278:** 51937–51949

Görlich D, Seewald MJ, Ribbeck K (2003) Characterization of Ran-driven cargo transport and the RanGTPase system by kinetic measurements and computer simulation. *EMBO J* **22:** 1088–1100

Guan T, Kehlenbach RH, Schirmer EC, Kehlenbach A, Fan F, Clurman BE, Arnheim N, Gerace L (2000) Nup50, a nucleoplasmically oriented nucleoporin with a role in nuclear protein export. *Mol Cell Biol* **20:** 5619–5630

Hodel MR, Corbett AH, Hodel AE (2001) Dissection of a nuclear localization signal. *J Biol Chem* **276:** 1317–1325

Hood JK, Casolari JM, Silver PA (2000) Nup2p is located on the nuclear side of the nuclear pore complex and coordinates Srp1p/importin-α export. *J Cell Sci* **113:** 1471–1480

Jones TA, Cowan S, Kjelgaard M (1991) Improved methods for building protein models in electron density maps and the location of errors in these models. *Acta Crystallogr A* **47:** 110–119

Kobe B (1999) Autoinhibition by an internal nuclear localization signal revealed by the crystal structure of mammalian importin α. *Nat Struct Biol* **6:** 388–397

Kraulis PJ (1991) MOLSCRIPT: a program to produce both detailed and schematic plots of protein structures. *J Appl Crystallogr* **24:** 946–950

Lee SJ, Matsuura Y, Liu SM, Stewart M (2005) Structural basis for nuclear import complex dissociation by RanGTP. *Nature* **435:** 693–696

Lindsay ME, Plafker K, Smith AE, Clurman BE, Macara IG (2002) Npap60/Nup50 is a tri-stable switch that stimulates importin-α:β-mediated nuclear protein import. *Cell* **110:** 349–360

Matsuura Y, Lange A, Harreman MT, Corbett AH, Stewart M (2003) Structural basis for Nup2p function in cargo release and karyopherin recycling in nuclear import. *EMBO J* **22:** 5358–5369

Matsuura Y, Stewart M (2004) Structural basis for the assembly of a nuclear export complex. *Nature* **432:** 872–877

Merritt EA, Bacon DJ (1997) Raster3D: photorealistic molecular graphics. *Methods Enzymol* **277:** 505–524

Nicholls A, Sharp KA, Honig B (1991) Protein folding and association: insights from the interfacial and thermodynamic properties of hydrocarbons. *Proteins: Struct Funct Genet* **11:** 281–296

Perrakis A, Morris R, Lamzin VS (1999) Automated protein model building combined with iterative structure refinement. *Nat Struct Biol* **6:** 458–463

Rabut G, Doye V, Ellenberg J (2004) Mapping the dynamic organization of the nuclear pore complex inside single living cells. *Nat Cell Biol* **6:** 1114–1121

Solsbacher J, Maurer P, Vogel F, Schlenstedt G (2000) Nup2, a yeast nucleoporin, functions in bidirectional transport of importin α. *Mol Cell Biol* **20:** 8468–8479

Vetter IR, Arndt A, Kutay U, Gorlich D, Wittinghofer A (1999) Structural view of the Ran-importin b interaction at 2.3 Å resolution. *Cell* **97:** 635–646

Weis K (2003) Regulating access to the genome. Nucleocytoplasmic transport throughout the cell cycle. *Cell* **112:** 441–451

Yang F, Moss LG, Phillips GN (1996) The molecular structure of green fluorescent protein. *Nat Biotechnol* **14:** 1246–1251

Yang W, Gelles J, Musser SM (2004) Imaging of single-molecule translocation through nuclear pore complexes. *Proc Natl Acad Sci USA* **101:** 12887–12892

Zeitler B, Weis K (2004) The FG-repeat asymmetry of the nuclear pore complex is dispensable for bulk nucleocytoplasmic transport *in vivo*. *J Cell Biol* **167:** 583–590